CHAPTER 18

Performance of the Neumann-Dirichlet Preconditioner for Substructures with Intersecting Interfaces

Włodzimierz Proskurowski*
Saliha Sha*

Abstract. There is indication that the Neumann-Dirichlet preconditioner for substructures with intersecting interfaces performs erratically for strongly discontinuous coefficients. The present work investigates the cause for such a behavior.

Introduction. Results in [2] indicated that the Neumann-Dirichlet preconditioner for substructures with intersecting interfaces works well even in some cases when sharp discontinuities of the coefficients at the interfaces are present. Experimental evidence in [4] shows that, in general, the iterations in which this preconditioner is employed converge unsatisfactorily slowly. Since the method works well for some discontinuous coefficients but not for some others we engaged in this study to determine the source of the difficulties. We, therefore, started a process of backtracking the effects of the method on increasingly more complex problems. We thus monitored the properties of the capacitance matrix and the rate of convergence of the corresponding iterations. As the main experimental tool we used MATLAB run on the SUN 3/260 computer with the precision of about 1e-14. This paper presents the logbook of our investigations.
We first examine the spectral distribution of the capacitance matrix for the Neumann-Dirichlet preconditioner with intersecting interfaces for the model problem with continuous and discontinuous coefficients in subregions (in [6] similar preconditioners with non-intersecting interfaces were considered). Next, we study the performance of the preconditioned conjugate gradient iterations for such capacitance matrix systems.

* Dept. of Mathematics, Univ. of Southern California, Los Angeles, CA 90089-1113.

Neumann-Dirichlet preconditioners. Let us consider two dimensional elliptic problems with self-adjoint operators

$$- \mathrm{div}(k(x,y)\mathrm{grad}u) = f(x,y) \quad \text{in } \Omega = (0,1)x(0,1) \tag{1}$$

with Dirichlet boundary conditions at $\partial\Omega$. We use the standard second order accurate staggered grid approximation that gives rise to a symmetric matrix representation A;

For i,j=1,...,n-1:

$$-(k_{i+1/2,j-1/2}+k_{i+1/2,j+1/2})u_{i+1,j}-(k_{i-1/2,j-1/2}+k_{i+1/2,j-1/2})u_{i,j-1}$$
$$-(k_{i-1/2,j+1/2}+k_{i+1/2,j+1/2})u_{i,j+1}-(k_{i-1/2,j-1/2}+k_{i-1/2,j+1/2})u_{i-1,j}$$
$$+2(k_{i-1/2,j-1/2}+k_{i-1/2,j+1/2}+k_{i+1/2,j-1/2}+k_{i+1/2,j+1/2})u_{i,j}=2h^2f_{i,j}$$

It should be noted that the approximation by piecewise linear finite elements on regular triangles results in exactly the same matrix A.

In the case when k(x,y)=1, i.e. of the Laplace operator, the $(n-1)^2x(n-1)^2$ matrix A has the well known form (here, $(n-1)^2$ is the number of grid points inside Ω):

$$A = \begin{pmatrix} T & -I & & & \\ -I & T & -I & & \\ & \cdot & \cdot & \cdot & \\ & & -I & T & -I \\ & & & -I & T \end{pmatrix}, \qquad T = \begin{pmatrix} 4 & -1 & & & \\ -1 & 4 & -1 & & \\ & \cdot & \cdot & \cdot & \\ & & -1 & 4 & -1 \\ & & & -1 & 4 \end{pmatrix}.$$

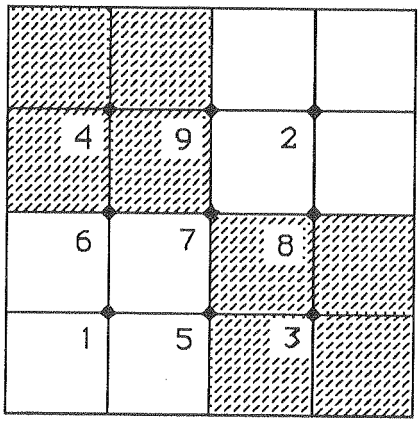

Fig.1

Let us now introduce a preconditioner, matrix B, constructed by imposing additional boundary conditions on the inner interfaces (or separators) in the following way. We divide Ω, here the unit square, with horizontal and vertical lines (interfaces) into N^2 subregions in a chessboard like manner (see Fig.1). We impose Neumann conditions on the boundary of the shaded subregions and Dirichlet conditions on the boundary of the remaining ones, and retain the original conditions on $\partial\Omega$. The $(N-1)^2$ points of intersection of the interfaces we shall call cross points. The total number of grid points on the interfaces is equal to $p=2(n-1)(N-1)-(N-1)^2$. Thus, p is much smaller than n^2.

After reordering, matrices A and B can be represented in a block form as:

$$A=\begin{bmatrix} A_{11} & 0 & A_{13} \\ 0 & A_{22} & A_{23} \\ A_{31} & A_{32} & A_{33} \end{bmatrix}, \quad B=\begin{bmatrix} A_{11} & 0 & A_{13} \\ 0 & A_{22} & A_{23} \\ 0 & B_{32} & B_{33} \end{bmatrix} \tag{2}$$

where the block-rows correspond to the Dirichlet subregions, Neumann subregions, and the interfaces. We retain the same staggered grid approximation as in A and approximate the Neumann boundary conditions by the second order central difference, i.e., when $k(x,y)=1$, $B_{33}=A_{33}$ and $B_{32}=2A_{32}$. In this case, finite elements produce matrix B with the third block-row scaled by 1/2 that has identical spectral properties.

$$B=\left(\begin{array}{cc|cc|ccccc} 4 & & & & -1 & -1 & & & \\ & 4 & & & & & & -1 & -1 \\ \hline & & 4 & & -1 & & & -1 & \\ & & & 4 & & -1 & & & -1 \\ \hline & & -2 & & 4 & & -1 & & \\ & & & -2 & & 4 & -1 & & \\ & & & & -1 & -1 & 4 & -1 & -1 \\ & & -2 & & & & -1 & 4 & \\ & & & -2 & & & -1 & & 4 \end{array}\right) \tag{3}$$

In the simplest case of only four subregions (N=2 and n=4, see Fig.1) matrix B has the form (3).

In general, B can be used as an efficient preconditioner for A if it satisfies the two principal conditions:

a) a system with B is easily solvable (relatively to that with A),

b) the spectrum of AB^{-1} is well conditioned.

Additionally, the existence of a cluster of eigenvalues away from zero is advantageous. Questions concerned with the first condition were addressed in [2] (for its parallel implementation see also [3]).

The second condition is best satisfied if A and B are spectrally equivalent. The method of domain decomposition often can be considered as a process in a subspace. This amounts to performing the main iteration for the system with the pxp capacitance matrix C of the form:

$$C=S^TAB^{-1}S,$$

where S^T is the restriction operator $S^T=(0, 0, I_p)$.

Thus, it is sufficient to require that A and B are spectrally equivalent in a subspace:

$$a_1x^TS^TASx \le x^TS^TBSx \le a_2x^TS^TASx$$

where the constants a_1 and a_2 are independent of the grid size parameter h=1/n. In practice, it suffices if they are at most weakly (logarithmically) dependent on h.

It can also be shown, see [1], that $C = C_1C_2^{-1}$, where the Schur complements of A and B are defined as follows:

$$\begin{aligned} C_1 &\equiv (S^TA^{-1}S)^{-1} = A_{33} - A_{31}A_{11}^{-1}A_{13} - A_{32}A_{22}^{-1}A_{23} \\ C_2 &\equiv (S^TB^{-1}S)^{-1} = B_{33} - B_{31}A_{11}^{-1}A_{13} - B_{32}A_{22}^{-1}A_{23} \end{aligned} \qquad (4)$$

Obviously, if A and B are symmetric positive definite, so are C_1 and C_2. The capacitance matrix C is nonsymmetric, in general. Nevertheless, if C_1 and C_2 remain symmetric then all eigenvalues of C are real, since C is similar to $C_2^{-1/2}C_1C_2^{-1/2}$:

$$\begin{aligned} &C\phi = C_1C_2^{-1}\phi = \lambda\phi, \quad C_2^{-1/2}C_1C_2^{-1/2}\varphi = \lambda\varphi, \qquad (5) \\ &\text{where} \quad C_2^{-1/2}\phi = \varphi. \end{aligned}$$

Theoretical predictions about the behavior of the Neumann-Dirichlet preconditioner for a large class of elliptic operators were presented in [7]. They show that the spectral bound a_2/a_1 equals to $O(1+\log^2(n/N))$, i.e. is a very slow growing function of the ratio of the numbers of grid points to subregions.

We verify this prediction experimentally by examining the condition number of the capacitance matrix, $\kappa(C)$, and then check the correlation between $\kappa(C)$ and the rate of convergence of the preconditioned conjugate gradient iterations measured by the number of iterations required for convergence. It should be noted that some estimates of $\kappa(C)$ were obtained previously in [2] and [3]. The results reported below were computed using MATLAB.

Condition number of the capacitance matrix. In contrast to the situation with non-intersecting interfaces, see [6], even for the simplest case of four subregions (N=2 and n=4) the capacitance matrix is not equal to the unity, namely:

$$C = I + \frac{1}{96}R, \qquad R = \begin{pmatrix} 1 & -7 & 0 & 7 & -1 \\ -7 & 1 & 0 & -1 & 7 \\ 0 & 0 & 0 & 0 & 0 \\ 7 & -1 & 0 & 1 & -7 \\ -1 & 7 & 0 & -7 & 1 \end{pmatrix}, \tag{6}$$

The eigenvalues of R are 16, -12, and a triple zero eigenvalue (thus, the condition number of the capacitance matrix is $\kappa(C)=\frac{1+\frac{1}{6}}{1-\frac{1}{8}} = \frac{4}{3}$). This observation about the existence of many multiple unity eigenvalues of the capacitance matrix was found to be true also for all other values of n and N. In fact, the number of multiple unity eigenvalues is equal to $s=p-(N^2 - c)(n/N - 1)$, where p is the total number of eigenvalues, $p=2(n-1)(N-1)-(N-1)^2$, c=2 for N even, and c=1 for N odd.

It is interesting to see the similarity of C_1 and C_2 here (N=2 and n=4):

$$C_1 = \frac{1}{4}\begin{pmatrix} 14 & -1 & -4 & -1 & 0 \\ -1 & 14 & -4 & 0 & -1 \\ -4 & -4 & 16 & -4 & -4 \\ -1 & 0 & -4 & 14 & -1 \\ 0 & -1 & -4 & -1 & 14 \end{pmatrix}, \quad C_2 = \frac{1}{4}\begin{pmatrix} 14 & 0 & -4 & -2 & 0 \\ 0 & 14 & -4 & 0 & -2 \\ -4 & -4 & 16 & -4 & -4 \\ -2 & 0 & -4 & 14 & 0 \\ 0 & -2 & -4 & 0 & 14 \end{pmatrix} \tag{6'}$$

Table 1 demonstrates the dependence of the condition number of the capacitance matrix, $\kappa(C)$, on the number of grid points, n, and subregions, N.

N\n	4	8	16	18	20	24	30	32
2	1.33	1.95	2.76	2.91	3.05	3.30	3.63	3.72
4	-	2.71	4.76	-	5.58	6.30	-	7.52
6	-	-	-	4.02	-	4.99	5.82	-
8	-	-	2.93	-	-	4.10	-	5.08
10	-	-	-	-	2.96	-	4.14	-
12	-	-	-	-	-	2.97	-	-

Table 1. Condition number of the capacitance matrix, $\kappa(C)$, versus n and N.

The largest size of the capacitance matrix reported here is p=441 (for n=30 and N=10). For convenience, in Table 2, we tabulate the values of p for the range of experiments presented above.

N\n	4	8	16	18	20	24	30	32
2	5	13	29	33	37	45	57	61
4	-	33	81	-	105	129	-	177
6	-	-	-	85	-	145	205	-
8	-	-	161	-	-	273	-	385
10	-	-	-	-	261	-	441	-
12	-	-	-	-	-	385	-	-

Table 2. The size of the capacitance matrix, p, versus n and N.

As the results in Table 1 show, the condition number of the capacitance matrix is changing very slowly with the size of the matrix, and more precisely, with the values of n and N. The next figures illustrate the dependence of $\kappa(C)$ on n (Fig.2) and N (Fig.3). Clearly, for N>3, the more subregions, N, the smaller the condition number, $\kappa(C)$. At the same time, $\kappa(C)$ grows with n, the number of grids in an almost linear fashion.

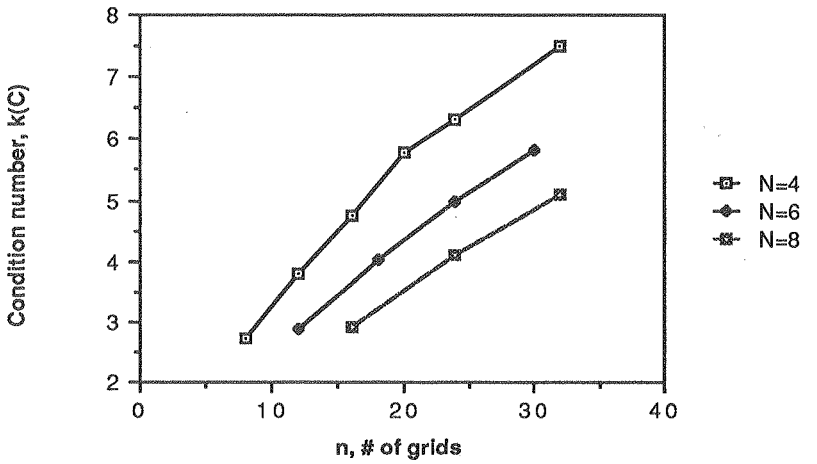

Fig.2. Condition number, $\kappa(C)$, versus the number of grids, n.

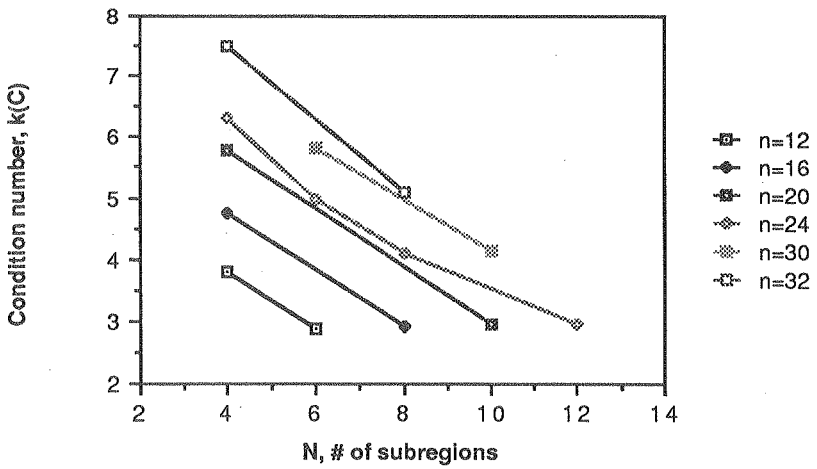

Fig.3. Condition number, $\kappa(C)$, versus the number of subregions,N.

From theoretical considerations, see for example [7], we expect $\kappa(C)$ to be proportional to $\log^2(n/N)$: $\kappa(C)=(a+b\log_{10}(n/N))^2$. For our data this is verified graphically in Fig.4. Here, the slopes b are almost identical and lie in the range (1.78, 1.80). The spectra of the capacitance matrices are indeed heavily clustered about 1. Thus, for example, for n=32 and N=4, out of the total of p=177 eigenvalues 129 of them lie in the interval (0.99,1.01).

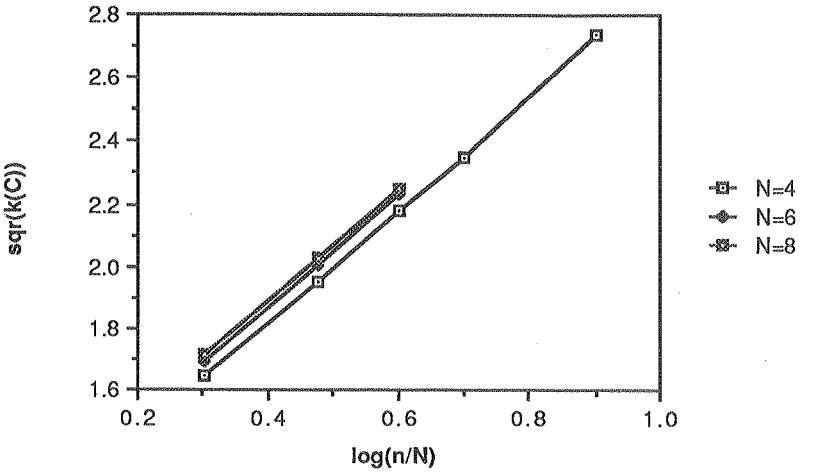

Fig.4. $\sqrt{\kappa(C)}$ *versus* $\log_{10}(n / N)$.

Discontinuous coefficients. Let us now consider problems where the diffusion function k(x,y) in (1) is discontinuous at all the interfaces and constant in each of the subdomains. We first discuss the simpler case where in all the Neumann subdomains $k(x,y)=c_1$ and in all the Dirichlet subdomains $k(x,y)=c_2$. For simplicity, we scale the problem using $c_2=1$ and we then vary $c_1 \equiv c$ from 10^{-5} to 10^5.

In the simplest case of four subregions (N=2 and n=4) and c=5, matrix B has the form:

$$B = \left(\begin{array}{cc|cc} 4 & & -1 & -1 \\ & 4 & & -1 & -1 \\ \hline & & 20 & & -5 & & -5 \\ & & & 20 & & -5 & & -5 \\ \hline & & -6 & & 12 & & -3 \\ & & & -6 & & 12 & -3 \\ & & & & -3 & -3 & 12 & -3 & -3 \\ & & -6 & & & & -3 & 12 \\ & & & -6 & & & & -3 & & 12 \end{array}\right) \qquad (7)$$

Matrices A and B have now the following block-form similar to (2) where, again, with the use of finite elements the third block row of B is scaled so that $B_{32} = B_{23}^T$.

$$A = \begin{bmatrix} A_{11} & 0 & A_{13} \\ 0 & cA_{22} & cA_{23} \\ A_{31} & cA_{32} & sA_{33} \end{bmatrix}, \quad B = \begin{bmatrix} A_{11} & 0 & A_{13} \\ 0 & cA_{22} & cA_{23} \\ 0 & 2sB_{32} & sB_{33} \end{bmatrix}, \quad \text{where } s = \frac{c+1}{2}. \tag{9}$$

In this case, the capacitance matrix has the form analogous to (6):

$$C = I + \frac{1}{48(c+1)}R, \qquad R = \begin{pmatrix} 1 & -7 & 0 & 7 & -1 \\ -7 & 1 & 0 & -1 & 7 \\ 0 & 0 & 0 & 0 & 0 \\ 7 & -1 & 0 & 1 & -7 \\ -1 & 7 & 0 & -7 & 1 \end{pmatrix} \tag{8}$$

Its condition number is $\kappa(C) = \frac{1+\frac{1}{3(c+1)}}{1-\frac{1}{4(c+1)}}$. When $c \to 0$, $\kappa(C) \to \frac{16}{9} \approx 1.778$.

The results of some of the experiments are tabulated below. (Table 3)

	N=4					n=24		
c	n=8	n=12	n=16	n=24	n=32	N=4	N=6	N=8
10^{-5}	7.332	14.55	22.66	39.63	56.51	39.63	24.90	16.80
10^{-4}	7.331	14.54	22.65	39.60	56.46	39.60	24.88	16.80
10^{-3}	7.315	14.49	22.55	39.39	56.09	39.39	24.78	16.74
10^{-2}	7.158	14.05	21.67	37.34	52.62	37.34	23.76	16.18
10^{-1}	5.983	10.81	15.67	24.71	32.68	24.71	16.94	12.21
0.3	4.484	7.317	9.920	14.37	18.05	14.37	10.57	8.088
1	2.708	3.814	4.760	6.295	7.517	6.295	4.990	4.099
3	1.694	2.089	2.417	2.943	3.357	2.943	2.496	2.189
10	1.226	1.346	1.446	1.604	1.729	1.604	1.470	1.376
10^2	1.023	1.035	1.045	1.061	1.074	1.061	1.048	1.039
10^3	1.002	1.004	1.005	1.006	1.007	1.006	1.005	1.004
10^4	1.000	1.000	1.000	1.001	1.001	1.001	1.001	1.001

Table 3. Condition number, κ(C), as a function of the ratio of diffusion coefficients, c; first for N=4 and different n, then for n=24 and different N.

We plot these results, first as a function of the number of subregions, N (Fig.5), then as a function of the number of grids, n (Fig.6).

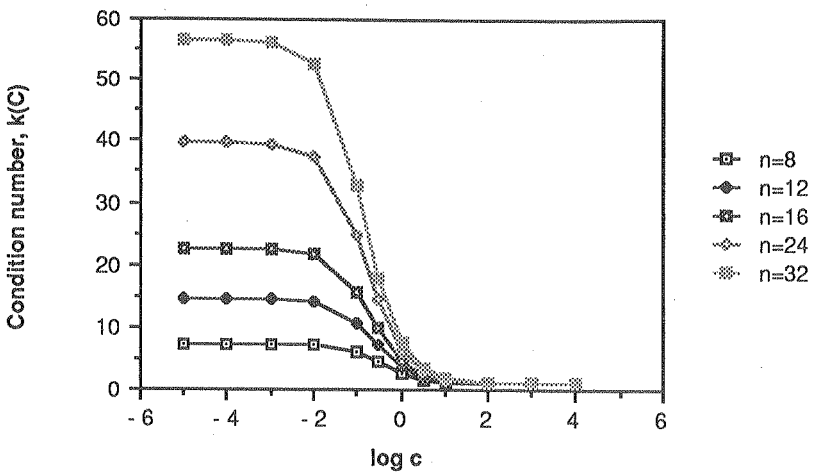

Fig.5. Condition number, κ(C), versus the log of the ratio of coefficients, c, for N=4.

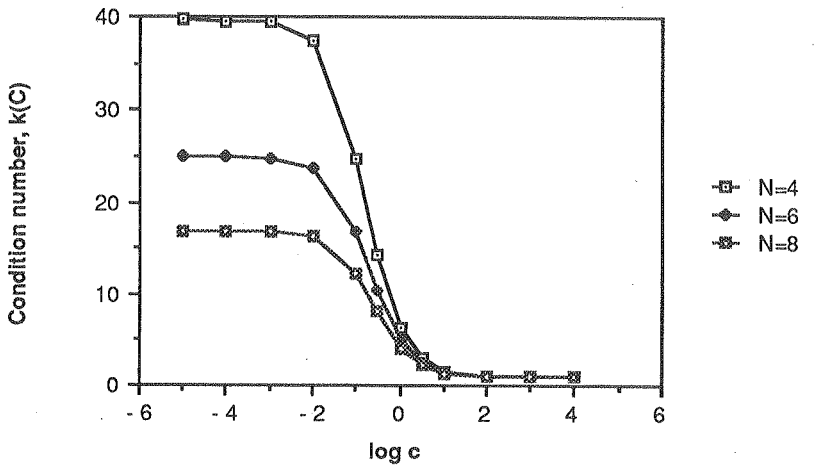

Fig.6. Condition number, κ(C), vs. the log of the ratio of coefficients, c, for n=24.

As is readily seen from these plots, in the two limiting cases: i/ κ(C) approaches the value of one when c approaches infinity, and ii/ κ(C) approaches a much higher value when c approaches zero. The first case corresponds to the situation when c is much larger in the Neumann subregions, the second to the one when c is much larger in the Dirichlet subregions.

We study in some detail the second case in order to develop from the experimental data an empirical formula of dependence of κ(C) on log(n/N). The results of experiments for $c=10^{-5}$ are given below. (Table 4)

$\frac{n}{N}$ =	2	3	4	5	6	8
N=4	7.33	14.55	22.66	31.42	39.63	56.51
N=6	8.26	16.18	24.90	33.88	-	-
N=8	8.59	16.80	-	-	-	-

Table 4. Condition number, $\kappa(C)$, for $c=10^{-5}$ and different values of n and N.

Based on this data, we conjuncture that $\kappa(C)$ is proportional to the fourth power of the logarithm of (n/N): $\kappa(C)=(a+b\log_{10}(n/N))^4$. This is verified graphically in Fig.7. Here again, as in Fig.4, the slopes b are almost identical and lie in the range (1.77, 1.82).

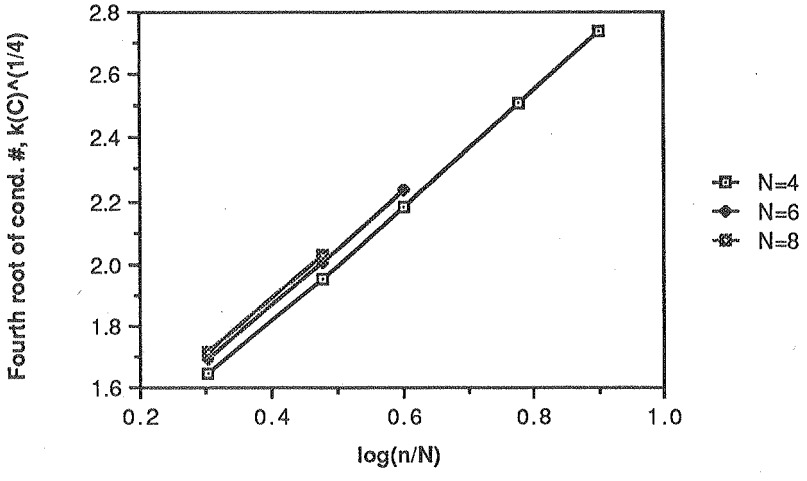

Fig.7. $\sqrt[4]{\kappa(C)}$ versus $\log_{10}(n/N)$ for the ratio of diffusion coefficients $c=10^{-5}$.

This conjecture can easily be proven using the idea suggested by Yuri Kuznetsov [5]. Consider the generalized eigenvalue problem

$$\lambda Bv = Av,$$

where A and B are as in (9). Then

$$\lambda = \frac{k_2 + k_1\mu}{k_2 + k_1},$$

where μ is the eigenvalue for the problem with continuous coefficients:

$$\mu(A_{33} - 2A_{32}A_{22}^{-1}A_{23})v_3 = (A_{33} - 2A_{31}A_{11}^{-1}A_{13})v_3.$$

Using the symmetry and antisymmetry of the eigenfunctions along the diagonals for the Laplacian on the unit square partitioned in a chessboard manner into Neumann and Dirichlet subregions, only the following four cases need to be examined:

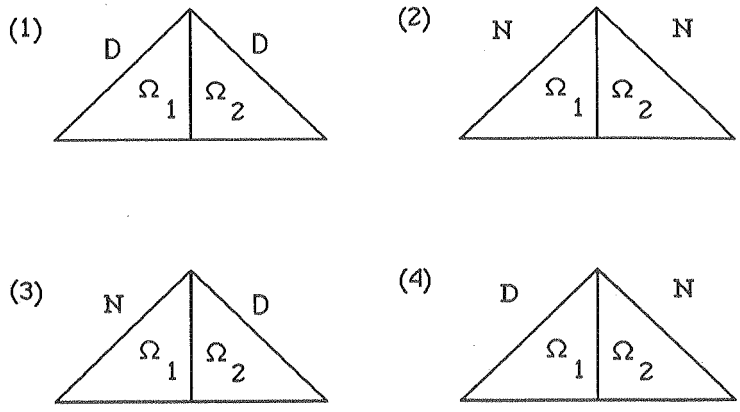

Cases 1 and 2 are benign with all eigenvalues $\mu=1=\lambda$.

In the cases 3 and 4 we have the estimates: (3) $1 \le \mu \le \varphi$, and (4) $\frac{1}{\varphi} \le \tilde{\mu} \le 1$,

where $\varphi = O(1+\log^2(n/N))$, see, for example, [7].

$$\text{Thus, } \lambda_{min} = \frac{k_2 + k_1 \mu_{min}}{k_2 + k_1} > \tilde{\mu}_{min} = \frac{1}{\varphi}, \text{ and}$$

$$\lambda_{max} = \frac{k_2 + k_1 \mu_{max}}{k_2 + k_1} \le \mu_{max} = \varphi.$$

Finally we obtain

$$\kappa(C) = \frac{\lambda_{max}}{\lambda_{min}} \le \frac{\mu_{max}}{\tilde{\mu}_{min}} = \varphi^2 = O(1+\log^4(n/N)),$$

independently of k_1 and k_2.

Irregular coefficients in subregions. Finally, we consider the case when diffusion coefficients, k, for each of the subregions are irregularly distributed. We focus our attention on the partition into 16 subregions, i.e. when N=4. This time the preconditioner matrices B are generated using solely finite elements since the use of finite differences gives rise to unsymmetric Schur complement matrices C_2.

Consider the magic square from the Albrecht Dürer's "Melancholia" painted in 1514:

$$\begin{pmatrix} 16 & 3 & 2 & 13 \\ 5 & 10 & 11 & 8 \\ 9 & 6 & 7 & 12 \\ 4 & 15 & 14 & 1 \end{pmatrix}$$

By dividing it by 4 and subtracting 2 we obtain the set of values for the initial 4x4 matrix of coefficients a_{ij} that is equidistantly distributed in [-2.0,1.75].

2.0	-1.25	-1.5	1.25
-0.75	0.5	0.75	0.0
0.25	-0.5	-0.25	1.0
-1.0	1.75	1.5	-1.75

Table 5. Distributed coefficients in subregions

In order to considerably vary these coefficients we apply the stretching transformation $a_{ij}^m = e^{ma_{ij}}$, where m=1,...,7. As a measure of discontinuity we use r, the ratio of the extreme diffusion coefficients in Ω: $r = \frac{\max a_{ij}^m}{\min a_{ij}^m}$..

The following table contains the results of experiments with this data. (Table 6)

m	r	n=8	n=12	n=16	n=20
1	4.25e+1	2.74e+1	3.07e+1	3.40e+1	3.71e+1
2	1.81e+3	6.88e+2	7.37e+2	7.89e+2	8.38e+2
3	7.69e+4	1.76e+4	1.86e+4	1.97e+4	2.07e+4
4	3.27e+6	4.53e+5	4.77e+5	5.02e+4	5.25e+4
5	1.39e+8	1.17e+7	1.22e+7	1.29e+7	1.34e+7
6	5.91e+9	3.01e+8	3.15e+8	3.30e+8	3.44e+8
7	2.51e+11	7.75e+9	8.11e+9	8.50e+9	8.86e+9

Table 6. Condition number, $\kappa(C)$, for irregularly distributed coefficients in subregions. Here, m is the exponential stretching factor and r is the ratio of the extreme coefficients.

This data demonstrates that in this case the condition number, $\kappa(C)$, grows rapidly (almost linearly) and unboundedly with r, where r is , while the dependence on the number of grids, n, is rather weak.

Preconditioned conjugate gradients. We now consider the solution of equation (1) using the preconditioned conjugate gradient iterations in which the Neumann-Dirichlet preconditioner, described in section 1, is employed. To solve a system with the capacitance matrix: Cw=b, we (formally) apply the conjugate gradient iterations to the transformed system

$$C_2^{-1/2} C_1 C_2^{-1/2} v = d, \quad \text{where} \quad v = C_2^{-1/2} w \quad \text{and} \quad d = C_2^{-1/2} b .$$

For the sake of completeness we summarize here the experimental results for the case of constant coefficients, i.e. k(x,y)=1, presented previously in [2] and [3]. In all the

experiments (the largest problem involved 256 subregions and about 16,000 unknowns) the initial guess was zero and the iterations were terminated when the energy norm, $\sqrt{r^T B^{-1} r}$, decreased 10,000 times, where, r is the residual .

N\n	32	48	64	96	128	32	48	64	96	128
4	7.08	8.79	10.1	12.1	13.6	7	8	8	8	8
6	-	7.54	-	10.8	-	-	9	-	10	-
8	4.91	6.39	7.68	9.56	11.0	8	8	9	9	9
12	-	4.92	-	7.63	-	-	7	-	9	-
16	-	4.01	4.94	6.45	7.65	-	7	7	8	9

Table 7. Estimates of the condition number, $\kappa(C)$, and number of conjugate gradient iterations versus n and N.

The number of iterations remains almost constant within the range of experiments and the estimates of the condition number of the capacitance matrix, $\kappa(C)$, obtained during conjugate gradient iterations are in good agreement with those results in Table 1 where they overlap.

We also performed a series of experiments for problems with discontinuous diffusion coefficients k(x,y). As before, we first discuss the simplest case where the constant k in all the Neumann subdomains varies from 10^{-4} to 10^{3} , and k=1 in all the Dirichlet subdomains. The results for 16 subdomains (N=4) are tabulated and plotted below. (Fig. 8 and Table 8)

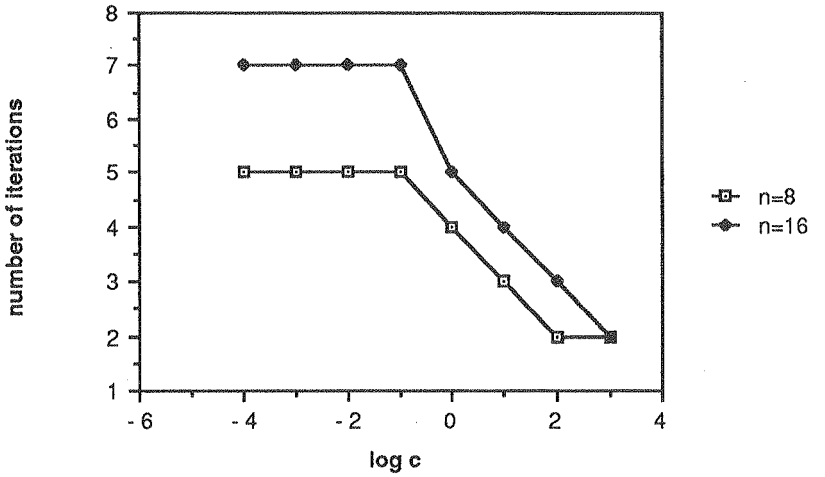

Fig.8. Number of iterations versus the log of the ratio of coefficients, c, for N=4.

log c =	-4	-3	-2	-1	-.5	0	.5	1	2	3
n=8	5	5	5	5	5	4	4	3	2	2
n=16	7	7	7	7	6	5	4	4	3	2
n=24	8	8	8	7	6	5	5	4	3	2

Table 8. Number of iterations versus the log of the ratio of coefficients, c, for N=4.

The rate of convergence of the conjugate gradient iterations changes smoothly with c, the ratio of coefficients, and essentially does not grow when this ratio becomes less than 0.01. This is consistent with the behavior of the condition number, $\kappa(C)$, as a function of c (see Figs. 5 and 6).

Next we performed the experiments using the irregularly the distributed coefficients in 16 subregions (N=4), see Tables 5 and 6.

m	r	n=8	n=12	n=16	n=20
1	4.25e+1	12	15	17	17
2	1.81e+3	13	19	28	28
3	7.69e+4	11	18	25	27
4	3.27e+6	7	10	15	11
5	1.39e+8	5	8	10	11
6	5.91e+9	4	5	7	7
7	2.51e+11	4	5	6	7

Table 9. Number of iterations for irregularly distributed coefficients in subregions.

To better understand the erratic behavior of the iterations let us focus our attention on the simplest case of four subregions (N=2). We choose the 2x2 matrix of diffusion coefficients as:

$$\begin{pmatrix} 1 & 2^{-i} \\ 2^{i} & 1 \end{pmatrix}$$

with i=0, 1, 2, ... where the coefficients equal to 1 are situated in the Neumann subregions. With this construction, only the triangles that belong to the Neumann subregions contribute to the elements of matrix B corresponding to the points on the interfaces. Thus, the Schur complement matrices C_2 remain unchanged when we vary the coefficients (i=0, 1, 2, ...) in the Dirichlet subregions; at the same time the Schur complement matrices C_1 change dramatically. As a consequence, matrices C_1 and C_2 for strongly dicontinuous coefficients are no longer similar, thus obviously not

spectrally equivalent either. To illustrate the point we present the results of some experiments (see (6') for the case i=0), first for i=1 then for i=10:

$$C_1 = \frac{1}{8}\begin{pmatrix} 42 & -2 & -12 & -4 & 0 \\ -2 & 21 & -6 & 0 & -1 \\ -12 & -6 & 36 & -12 & -6 \\ -4 & 0 & -12 & 42 & -2 \\ 0 & -1 & -6 & -2 & 21 \end{pmatrix}, \quad C_1 = \frac{10^6}{4092}\begin{pmatrix} .007 & -.001 & -.002 & .0 & 0 \\ -.001 & 7.35 & -2.10 & 0 & -1.05 \\ -.002 & -2.10 & 4.20 & .002 & -2.10 \\ .0 & 0 & -.002 & .007 & -.001 \\ 0 & -1.05 & -2.10 & -.001 & 7.35 \end{pmatrix}$$

Finally we compile the table of results where the condition numbers of C and C_1 are compared while the discontinuity coefficients in the Dirichlet subregions increases. (Table 10)

i	0	1	2	3	4	10
$\kappa(C)$	1.33	2.35	4.67	9.34	18.7	1.19e+3
$\kappa(C_1)$	3.86	4.46	6.29	11.0	19.5	1.14e+3

Table 10. Condition numbers of C & C_1 depending on the discontinuity of coefficients.

Acknowledgments We would like to thank Max Dryja for comments on the manuscript.

References

[1] M.Dryja, SIAM J.Num.Anal., A finite element capacitance matrix method for elliptic problems, v.20, 1983, 671-680.

[2] M.Dryja, W.Proskurowski & O.Widlund, Numerical experiments & implementation of domain decomposition method with cross points, in *Advances in Computer Methods for PDEs -VI*, (R.Vichnevetsky & R.Stepleman, eds.), IMACS, 1987, 23-27.

[3] M.Haghoo & W.Proskurowski, Parallel implementation of a domain decomposi-tion method, in *Proc. 2nd Domain Decomposition Conf.* (T.Chan, ed.), SIAM, 1989.

[4] A.Greenbaum, C.Li & H.Chao, Comparison of linear system solvers applied to diffusion-type finite element eqns., Courant Inst. NYU, Ultracomp. Note #126, 1987.

[5] Yu.Kuznetsov, private communication, March 1989.

[6] W.Proskurowski, Remarks on spectral equivalence of certain discrete operators, in *Proc. Second Domain Decomposition Conf.* (eds. T.Chan et al.), SIAM, 1989.

[7] O.Widlund, Iterative substructuring methods: algorithms & theory for elliptic problems in plane, in *Proc. 1st Domain Decomposition Conf.* (R.Glowinski, ed.), SIAM, 1988, 113-128.